

Supplementary information for:

Mechanism of Ion Transfer in Supported Liquid Membrane Systems: Electrochemical Control over Membrane Distribution

Matěj Velický,[†] Kin Y. Tam,[‡] Robert A.W. Dryfe^{†}*

[†] School of Chemistry, University of Manchester, Oxford Road, Manchester M13 9PL, UK

[‡] Faculty of Health Science, University of Macau, Macau, China

* To whom correspondence should be addressed. Tel: +44 (0)161-306-4522; Fax: +44 (0)161-275-4598, e-mail: robert.dryfe@manchester.ac.uk.

Supplementary Information Abstract:

The additional results and discussion presented in the Supplementary Information include rhodamine B stability under UV-vis light (S-2), spectrophotovoltammetric study of the reversible membrane electrolyte concentration oscillations (S-3), co-transfer coupled to the analyte transfer occurring at the other ITIES (S-4), the effects of distribution/dissociation equilibrium of rhodamine B on transfer (S-5) and double transfer voltammograms for series of cations and anions (S-6).

S-2 Rhodamine B stability under UV-vis light

The stability of the molecule under UV light was confirmed by collecting the UV-vis spectra of a 2 μ M solution rhodamine B solution for 100 h as shown in Fig. S-2. Over the course of UV-vis irradiation and absorbance detection, the shape of the spectra was not changed and the overall absorbance decreased by a mere 1.5%, indicating the slight adsorption of RB on the walls of the lower PTFE cell, which was also visible as a slight colouring on the PTFE.

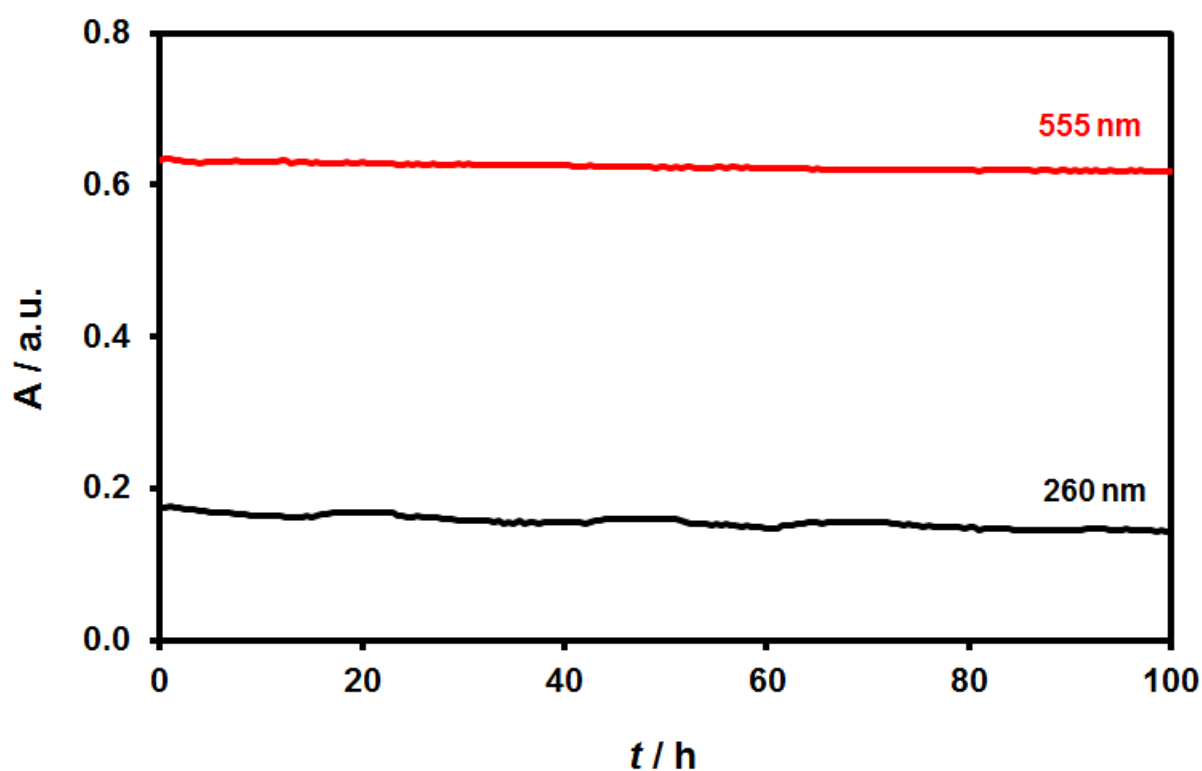


Figure S-2 UV-vis absorbance of 2 μ M rhodamine B aqueous solution measured with time to determine the molecule's stability under UV-vis light.

S-3 Spectrophotovoltammetry in an analyte-free SLM system

A blank supported liquid membrane system, containing only the organic solvent, aqueous buffer, and both aqueous and organic electrolytes, was analysed using cyclic voltammetry. The comparison of the voltammetric data obtained for 1-octanol, 1,9-decadiene, 1,2-dichlorobenzene and nitrophenyl octyl ether is shown in Fig. S-3a. With exception of 1-octanol, all solvents exhibit a large baseline potential window of about 1.2 V width (for $|I| < 2 \mu\text{A}$), centred around 0 V, which is suitable for transfer of ions within this potential range. The potential window is limited by the transfer of either tetradodecylammonium (TDDA^+) or tetrakis(4-chlorophenyl)borate (TPBCl_4^-) organic electrolyte ions, which both exit the membrane at extreme potentials depending on their standard transfer potential value. The phase to which the respective ions transfer depends on the polarity applied to the SLM as indicated in Fig. S-3a. Detailed voltammetric study using TDDACl and KTPBCl_4 as the membrane electrolytes has proven that TPBCl_4^- anion (rather than TDDA^+ cation) limits the potential window.¹ NPOE produces a very low and featureless current-potential response, which makes this solvent an excellent choice for electrochemical measurements in this SLM system. Both 1,9-decadiene and ODCB result in a large potential window comparable to NPOE but the current-potential response is inferior. 1-octanol, on the other hand, has a poor response with a potential window of a mere 0.4 V (for $|I| < 10 \mu\text{A}$) due to its high resistivity, which makes it an unsuitable system for electrochemical experiments in this configuration.

Rotation of the SLM about its vertical axis results in stable hydrodynamic conditions (including mixing of the aqueous phases) and enables reversible transfer of the electrolyte in and out of the membrane to be measured via UV-vis spectrophotometry simultaneously with the electrochemical measurement. Fig. S-3b shows the UV-vis absorbance of the aqueous phase B at wavelength 260 nm measured against time simultaneously with the cyclic voltammetry in the blank NPOE system. The changing absorbance indicates the appearance and disappearance of the TPBCl_4^- ion in the phase B. The average period of the pseudo-sinusoidal response is ~ 110 s, which corresponds to a potential sweep of

2.2 V (scan rate 20 mV s) and matches the period of cyclic voltammogram (2.2 V per scan) showing that the changes in absorbance follow the voltammetric sweeps. The fact that the oscillation period matches one full voltammetric cycle supports the assumption that only one type of ion transfers out of the membrane. In the case where both TPBCl_4^- and TDDA^+ transferred simultaneously, the periodicity would be halved (transfer from SLM to B would occur at each potential extreme) and the amplitude symmetry would be broken (as the ions have different absorbance). The transfer of TPBCl_4^- in and out of the membrane is, to a first approximation, reversible, which is demonstrated by the absorbance derivative plotted as a function of time in inset of Fig. S-3b. The absorbance derivative is related to the current response (both functions report on the ion flux) and its shape, *i.e.* symmetry about the time axis, indicates almost reversible transport in and out of the membrane.² The amplitude of the absorbance oscillations around the mean value correspond to changes in the TPBCl_4^- concentration of $\sim 0.2 \mu\text{M}$ around the mean concentration governed by the distribution equilibrium of TPBCl_4^- between the aqueous phase and SLM.¹ The mean absorbance value (dashed line in Fig. S-3b corresponding to concentration of $0.25 - 0.5 \mu\text{M}$), which slowly increases with time, reflects the subtle irreversibility of the ion transfer, *i.e.* fraction of the transferred ions lost in the bulk of the aqueous phases due to stirring. The first 400 s of the experiment, which are not shown, exhibited an unstable absorbance fluctuation attributed to the membrane loading effects described elsewhere.³

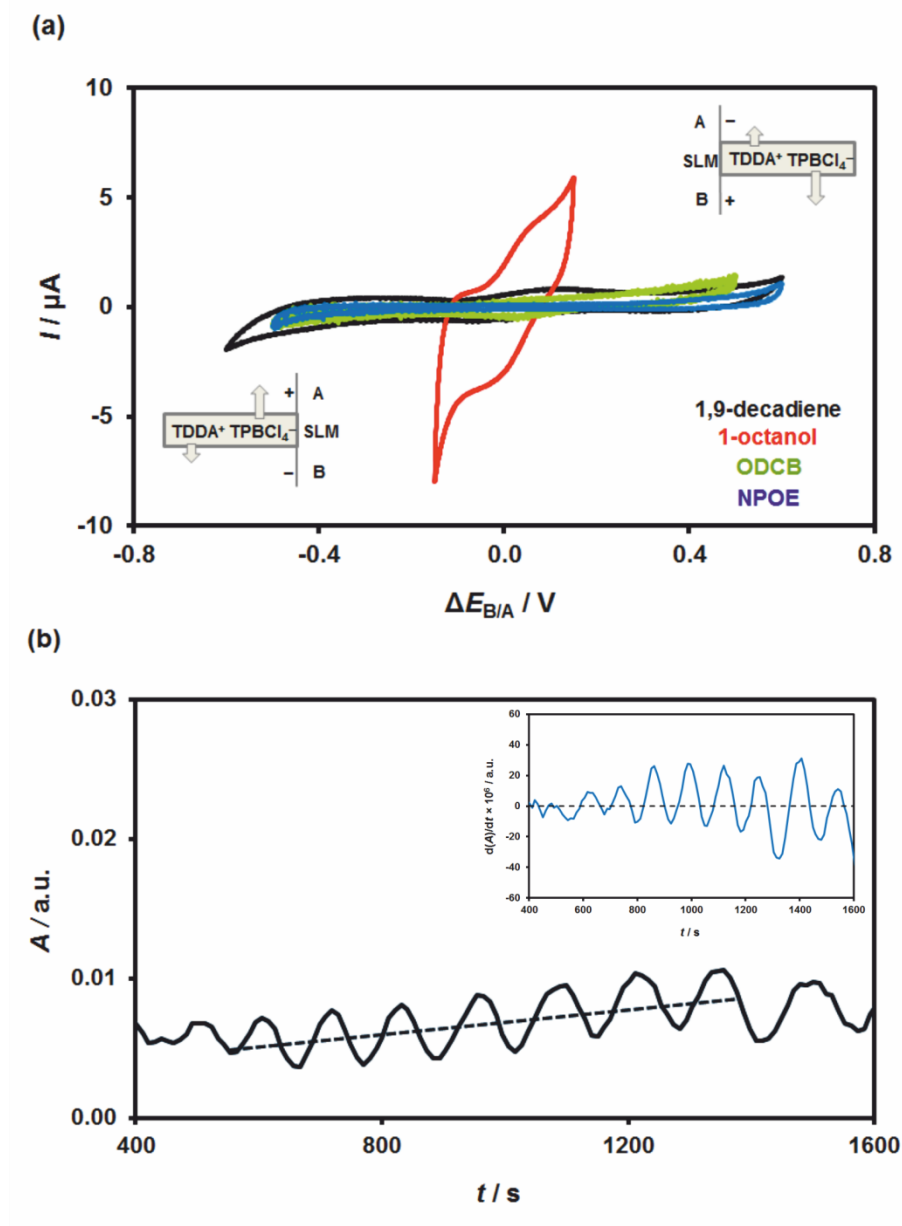
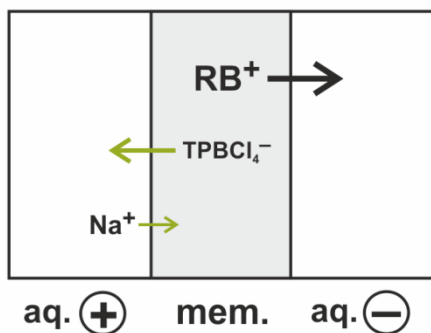


Figure S-3 (a) Cyclic voltammetry in a blank supported liquid membrane system. The current is recorded as a function of potential (applied potential difference) between phase B and phase A at a scan rate of 20 mV s^{-1} and membrane rotated at 200 rpm (21 rad s^{-1}). The direction of the voltammogram was toward negative potentials first with a starting potential of 0 V. Four different membrane solvents were used with respective IR compensation applied: black curve – 1,9-decadiene, 47 k Ω , red curve – 1-octanol, 9 k Ω , green curve – ODCB, 3.2 k Ω , blue curve – NPOE, 3 k Ω . (b) UV-vis absorbance recorded at wavelength 260 nm in phase B as a function of time simultaneously with cyclic voltammetry (NPOE SLM). The small inset shows the corresponding first derivative of the absorbance with time.

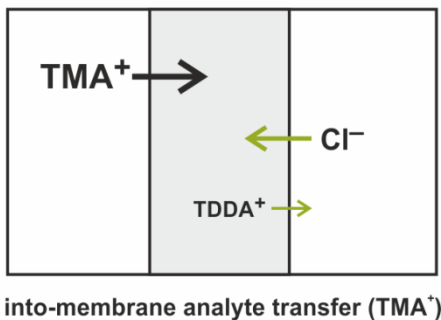
S-4 Analyte transfer coupling with co-transfer at the other ITIES

The transfer of the analyte across one of the ITIES has to be coupled with a transfer of another ion at the other interface in order to maintain the overall neutral charge of the bulk membrane phase. The ions transferring across both liquid-liquid interfaces induce excess positive or negative charge on each aqueous side of the membrane, which is detected via the pair of counter electrodes in the respective aqueous phases. Fig. S-4 demonstrates the possible routes of coupled co-transfer for out-of-membrane (a) and into-membrane (b) analyte transfer. The counter-ion identity is determined by its lipophilicity, *i.e.* the ion, which requires the least energy for the transfer across the ITIES will take part in the co-transport. The lipophilicity of the counter-ion also affects the transfer potential of the analyte as previously demonstrated by Kihara and co-workers.⁴ Fig. S-4a shows that both TPBCl_4^- or Na^+ ions can complement the transfer of rhodamine B ion out of the membrane. As shown in section S-3, transfer of TPBCl_4^- is observed at the limits of the potential window so this species is likely to be coupled with RB^+ transfer. The standard Gibbs energy of TPBCl_4^- transfer at NPOE/water interface (or in fact any other solvent) has not been reported, therefore a direct comparison of TPBCl_4^- or Na^+ lipophilicity is not possible. Nevertheless, the standard Gibbs energies of tetraphenylborate (TPB^-) and Na^+ transfer (NPOE/water) are known (-24.8 and 36.3 kJ mol^{-1} , respectively⁵) and assuming the TPBCl_4^- anion is only slightly more lipophilic than TPB^- it is reasonable to expect that TPBCl_4^- transfers at lower overpotentials than Na^+ . Same reasoning can be applied to the case of into-membrane direction of tetraalkylammonium transport (Fig.S-4b). The standard Gibbs energy of tetradodecylammonium cation transfer across NPOE/water interface, which has not been reported in literature, was estimated to be about -110 kJ mol^{-1} based on extrapolation of standard the Gibbs energies of tetra(-methyl,-ethyl, -propyl, -butyl and pentyl)ammonium cations.⁵⁻⁶ Therefore, the analyte transport into the membrane is coupled to chloride anion co-transfer (standard Gibbs energy of chloride transfer is 43.1 kJ mol^{-1} ⁵).

(a) out-of-membrane analyte transfer (RB^+)



(b)



into-membrane analyte transfer (TMA^+)

Figure S-4 Transport of cationic analytes in the SLM system coupled with co-transfer at the other ITIES. (a) rhodamine B out-of-membrane transfer coupled with TPBCl_4^- , (b) TMA^+ into-membrane transfer coupled with Cl^- .

S-5 Effects of partial ionisation of rhodamine B on membrane transfer

The case of fully ionized species B^+ is considered: as Fig. S-5 demonstrates, there is only one ionized transport ‘channel’ for B^+ to transfer between phases A, M and B. Therefore, changes in concentration on aqueous and membrane side of each interface are only affected by ionic flux induced by voltammetry (assuming steady-state permeation or concentration equilibrium). If this were the case for RB, one would expect the reverse peak current (aqueous-to-membrane) to be higher because the concentration change in each phase is of opposite sign and equal absolute value, whereas the diffusion in the aqueous phase is much faster thus resulting in larger peak current according to Eq. (4) (main text).

However, the observed reverse current, corresponding to transfer from the aqueous phases back to membrane (peak 2 and 4 in Fig. 4, main text) has a peak value 2 – 4 times smaller, depending on the solvent. This is consistent with the complex distribution/dissociation equilibrium occurring at liquid-liquid interface for partially ionized molecules,⁷ such as rhodamine B. As shown in Fig. S-5b, there are multiple transport ‘channels’, which the partially ionized molecule can take when transferring between the three phases. The decreased size of the reverse peak current can be rationalised as follows: the RB^+ cation is transferred from M to B upon applied potential difference (route 1 in Fig S-5b). When it reaches the aqueous phase B the dissociation equilibrium is rapidly established and converts the RB^+ ions to neutral RB (route 2 in Fig. S-5b) as $[RB^+]/[RB]$ is ~ 2000 at pH 7.0 at equilibrium. As a result, the available concentration of RB^+ ions in the aqueous phase B is lowered yielding a smaller reverse transfer peak current (route 3 in Fig. S-5b). The extent of this effect depends on the ratio between membrane and diffusion coefficients and difference in membrane and aqueous ionic concentration, both of which are specific to each membrane solvent. Stirring of the aqueous phase also has a lesser effect on this phenomenon.

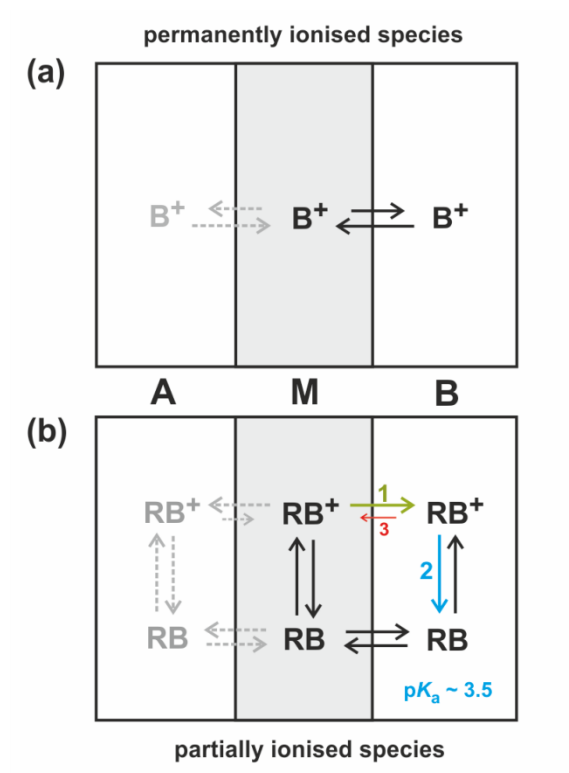


Figure S-5 Schematic diagram of (a) a simple distribution equilibrium of a permanently ionized ion B^+ . (b) complex distribution/dissociation equilibrium of the partially ionized species, rhodamine B. The coloured arrows represent the transfer routes of RB^+ cation during voltammetry.

S-6 Double-transfer voltammogram for a series of cations and anions

Fig. S-6 shows the cyclic voltammetric transfer data obtained for series of cations (S-6a) and anions (S-6b) to complement the data already presented in the main text. Table S-6 lists the half-wave potentials and peak separations for all studied cations and anions.

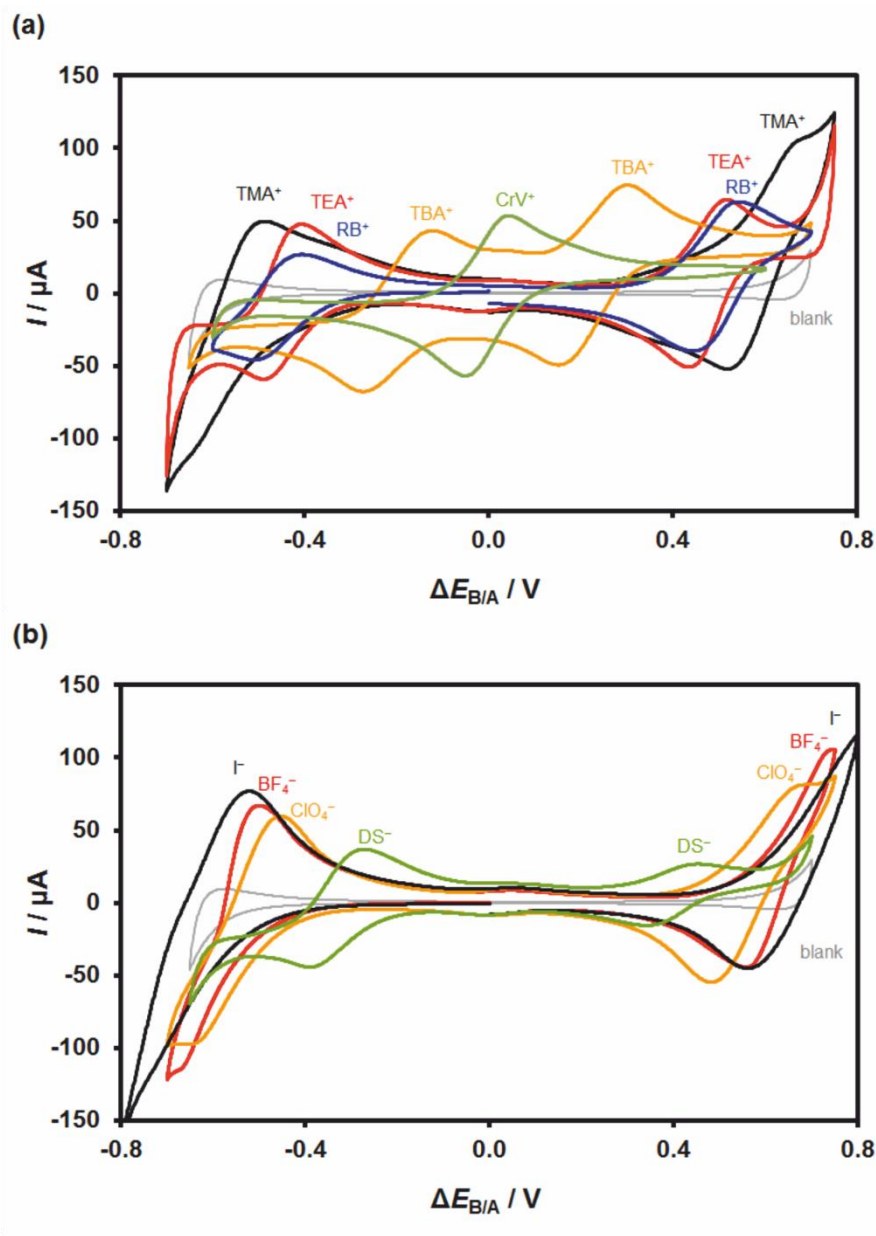


Figure S-6 Cyclic voltammograms of selected ions transferring across double-liquid interface in a NPOE supported liquid membrane system. (a) voltammograms of tetramethylammonium (black), tetraethylammonium (red), tetrabutylammonium (gold), crystal violet (green) and rhodamine B (blue). (b) voltammograms of iodide (black), tetrafluoroborate (red), iodide (gold) and dodecyl sulphate (green). Both aqueous phases were introduced with 1 mM concentration of the analyte (100 μM in the case of rhodamine B) with exception of crystal violet (1 mM concentration in phase A only). The grey curve is the analyte-free 'blank' voltammogram. Scan rate was 40 mV s^{-1} and the system was not stirred.

Table S-6 Half-wave potentials and peak separations of transfer of all the studied ions (obtained from 40 mV s⁻¹ scans).

ion	$E_i^{1/2} / \text{V}$		$\Delta E_p / \text{V}$	
	neg	pos	neg	pos
TMA ⁺	-0.558	0.594	0.131	0.136
TEA ⁺	-0.449	0.477	0.079	0.079
TBA ⁺	-0.198	0.227	0.148	0.149
RB ⁺ (only A)	-0.437	0.482	0.120	0.117
RB ⁺ (A and B)	-0.458	0.495	0.100	0.091
CrV ⁺	-0.004		0.092	
I ⁻	-0.631	0.655	0.218	0.190
BF ₄ ⁻	-0.587	0.647	0.171	0.179
ClO ₄ ⁻	-0.551	0.584	0.195	0.203
DS ⁻	-0.333	0.399	0.113	0.093

References

1. M. Velický. PhD Thesis, University of Manchester, 2011.
2. Z. Ding, R. G. Wellington, P. F. Brevet, H. H. Girault, *Journal of Electroanalytical Chemistry*. 1997, 420. 35-41.
3. M. Velický, D. F. Bradley, K. Y. Tam, R. A. W. Dryfe, *Pharmaceutical Research*. 2010, 27. 1644-1658.
4. O. Shirai, S. Kihara, Y. Yoshida, M. Matsui, *Journal of Electroanalytical Chemistry*. 1995, 389. 61-70.
5. L. A. J. Chrisstoffels, F. De Jong, D. N. Reinhoudt, *Chemistry - A European Journal*. 2000, 6. 1376-1385.
6. Z. Samec, J. Langmaier, A. Trojánek, *Journal of Electroanalytical Chemistry*. 1996, 409. 1-7.
7. M. Velický, K. Y. Tam, R. A. W. Dryfe, *Journal of Electroanalytical Chemistry*. 2012, 683. 94-102.